Journal of Cardiovascular Magnetic Resonance®, 1(3), 233–238 (1999)

Coronary Angiography

Breathhold Three-Dimensional Coronary Magnetic Resonance Angiography Using Real-Time Navigator Technology

Matthias Stuber,[1,2] René M. Botnar,[1,2] Peter G. Danias,[1] Kraig V. Kissinger,[1] and Warren J. Manning[1,3]

[1] *Cardiovascular Division and* [3] *Department of Radiology, Beth Israel Deaconess Medical Center and Harvard Medical School, Boston, Massachusetts*
[2] *Philips Medical Systems, Best, The Netherlands*

ABSTRACT

The acquisition duration of most three-dimensional (3D) coronary magnetic resonance angiography (MRA) techniques is considerably prolonged, thereby precluding breathholding as a mechanism to suppress respiratory motion artifacts. Splitting the acquired 3D volume into multiple subvolumes or slabs serves to shorten individual breathhold duration. Still, problems associated with misregistration due to inconsistent depths of expiration and diaphragmatic drift during sustained respiration remain to be resolved. We propose the combination of an ultrafast 3D coronary MRA imaging sequence with prospective real-time navigator technology, which allows correction of the measured volume position.

3D volume splitting using prospective real-time navigator technology, was successfully applied for 3D coronary MRA in five healthy individuals. An ultrafast 3D interleaved hybrid gradient-echo-planar imaging sequence, including T2Prep for contrast enhancement, was used with the navigator localized at the basal anterior wall of the left ventricle. A 9-cm-thick volume, with in-plane spatial resolution of 1.1 × 2.2 mm, was acquired during five breathholds of 15-sec duration each. Consistently, no evidence of misregistration was observed in the images. Extensive contiguous segments of the left anterior descending coronary artery (48 ± 18 mm) and the right coronary artery (75 ± 5 mm) could be visualized. This technique has the potential for screening for anomalous coronary arteries, making it well suited as part of a larger clinical MR examination. In addition, this technique may also be applied as a scout scan, which allows an accurate definition of imaging planes for subsequent high-resolution coronary MRA.

KEY WORDS: *Breathhold 3D coronary MRA; Real-time navigators; Ultrafast imaging.*

Received December 10, 1998; Accepted April 27, 1999
Address reprint requests to Matthias Stuber.

INTRODUCTION

Two-dimensional (2D) breathhold techniques have proven to be very powerful methods for coronary magnetic resonance angiography (MRA) (1–3). Still, three-dimensional (3D) coronary MRA offers the unique properties of thin adjacent slices, enhanced signal-to-noise ratio, and the superior postprocessing possibilities of a 3D data set (4–7). However, the acquisition duration of most 3D coronary MRA techniques is considerably increased, thereby precluding breathholding as a mechanism to suppress respiratory motion artifacts.

Such breathhold duration limitations may be overcome by splitting the 3D volume into multiple subvolumes, whereby each individual volume is asessed during a short end-expiratory breathhold interval (8,9). Because of inconsistent depths of sustained expiration, however, heart position may not be replicated in subsequent breathholds, causing registration errors (10,11). Furthermore, diaphragmatic drift has been reported during prolonged expiratory periods (12). Thus, blurring and/or discontinuities in the images may result. The use of prospective adaptive navigator correction is most effective in conjunction with breathhold splitting techniques (13,14).

We present a breathhold 3D coronary MRA technique in which the total 3D volume is split into smaller 3D slabs. Image data from each of those slabs are acquired in a relatively brief end-expiratory breathhold. To compensate for diaphragmatic drift or inconsistent depths of expiration (misregistration), a prospective real-time navigator-correction technique is applied (13,14).

MATERIALS AND METHODS

Multiple breathhold, real-time, navigator-corrected, 3D coronary MRA was performed in five healthy adult volunteers (three men and two women, aged 27 ± 7 yr). All measurements were performed on a Gyroscan ACS-NT 1.5-T whole body system (Philips Medical Systems, Best, NL) equipped with an advanced coronary software package and a PowerTrak 6000 gradient system (23 mT/m, 219-μsec rise time). For signal acquisition, a five-element commercial cardiac synergy coil was used.

Localizer

To localize the volume for 3D coronary MRA and to position the vertically oriented navigator at the basal anterior wall of the left ventricle, an electrocardiogram (ECG)-gated, segmented k-space, turbofield echo (TFE), scout scan of 10 coronal, 10 sagittal, and 10 transverse sections was used (TE, 1.8 msec, TR, 11 msec). All 30 slices were acquired in an interleaved mode during a 10 heart beat end-expiration breathhold.

3D Coronary MRA Sequence

For 3D coronary MRA, and ECG-gated, fat-suppressed, ultrafast interleaved gradient-echo-planar imaging sequence (TFE-EPI) was applied in a transverse plane (256 × 128 matrix, field of view 280 mm, four radiofrequency [RF] excitations per shot, EPI factor 7, TR 17 msec, TE 5 msec, RF excitation angle 30°, number of signal averages 1) (15). The measured slice thickness was 6 mm and the in-plane spatial resolution 1.1 × 2.2 mm. A schematic of the sequence elements used is displayed in Fig. 1.

For contrast enhancement between blood and myocardium, a T2 preparation (T2Pre-pulse) sequence was applied (16,17). The T2Pre-pulse (TE 50 msec) was followed by a regional saturation technique prepulse at the anterior chest wall, the navigator, and a spectral selective fat saturation prepulse. The 9-cm-thick transverse 3D volume (Fig. 2) was divided into five transverse overlapping units or slabs (9). The overlap of these subvolumes was 9 mm and a total of 30 slices of 3.0 mm thickness was calculated by interpolation during reconstruction. Each unit was acquired in a single end-expiratory sustained breathhold. Imaging was performed with ECG gating and an adjusted trigger delay (Fig. 1) to sample the image data in middiastole, a period of minimal bulk myocardial motion (18), and high coronary blood flow.

To compensate for the disadvantageous effects of inconsistent depths of expiration (misregistration) and diaphragmatic drift (12), a 2D selective vertically oriented navigator used for volume tracking (7) was localized at the base of the anterior wall of the left ventricle (Fig. 2). The navigator diameter was 12 mm, and 10 turns in k-space were used for navigator excitation. The navigator excitation angle was 30°. Dependent on the position of the navigator-detected lung–heart interface (Fig. 2), the superior–inferior (SI) position of the acquired volume is corrected prospectively in real time. Prospective adaptive slice correction (for a transverse slice orientation) in the SI direction is accomplished by changing the RF frequency of the selective excitation pulses ($\alpha_1 \ldots \alpha_n$, Fig. 1) of the imaged 3D volume. Because the navigator was positioned close to the proximal to midcoronary arteries (Fig. 2), a volume-tracking factor of 1.0 was applied (11). Correction was only performed in the SI direction.

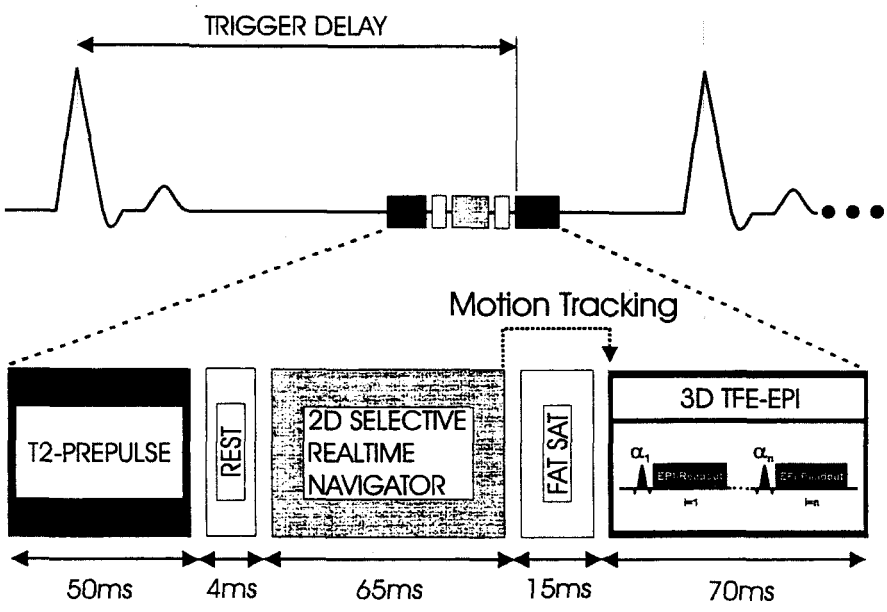

Figure 1. Schematic of the used sequence elements for breathheld 3D coronary MRA. The T2 prepulse (T2Prep) for contrast enhancement is followed by a local saturation prepulse (REST), a spectral selective fact saturation prepulse (FatSat), and the 3D interleaved segmented echo-planar imaging sequence. In the present implementation, $n = 4$ ($i = 1 \ldots n$) RF excitations ($\alpha_1 \ldots \alpha_4$) are followed by an EPI-readout train of seven echoes. The frequency of the slice-selective RF excitation pulses is adapted prospectively dependent on the navigator-detected position of the lung–heart interface.

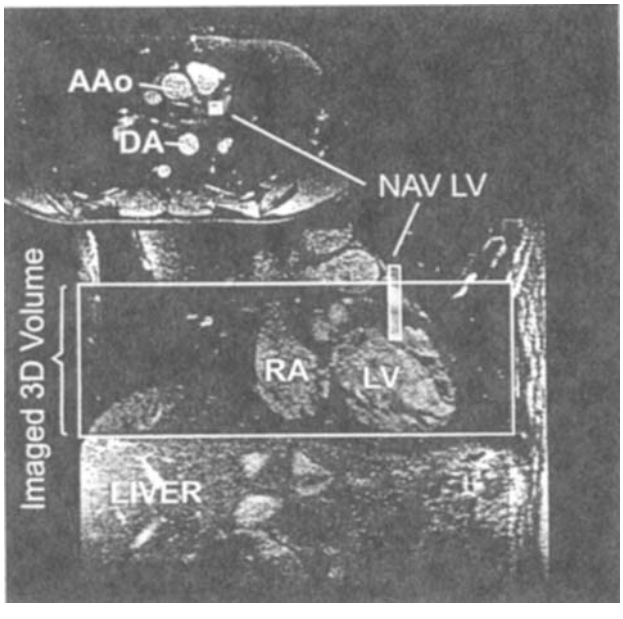

Figure 2. Localization of the 3D volume and the 2D selective navigator (NAV LV) at the anterior basal free wall of the left ventricle. AAo, ascending aorta; DA, descending aorta; RA, right atrium; LV, left ventricle.

3D Multiplanar Reformatting

After completion of the 3D coronary MRA scans in five breathholds, the image data were transferred to a commercially available EasyVision® workstation (Philips Medical Systems) for off-line reformatting of the 3D data set. During the reformatting process, the user navigates interactively in three perpendicular view of the acquired 3D data set. The coronary arteries are then identified by the user with an interactive mouse click. With this procedure, a series of points along the coronary vessel are specified in 3D. Subsequently, the image is reconstructed along the user-specified path and displayed in one plane with the "true" vessel dimensions (Figs. 3 and 4). Length measurements of the left main coronary artery (LM), the left anterior descending coronary artery (LAD), the left circumflex (LCX), and the right coronary artery (RCA) were subsequently performed on these reformatted images.

RESULTS

All scans were successfully completed without complications. A 3D volume of 9-cm thickness was acquired

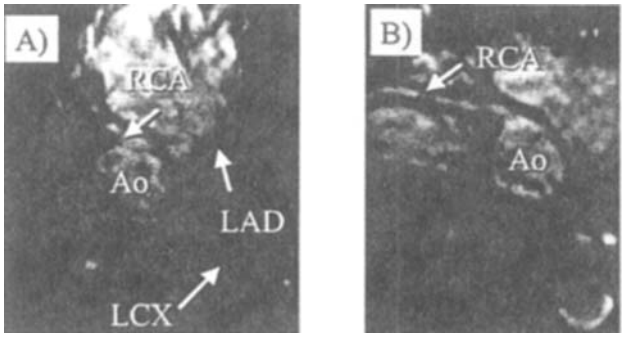

Figure 3. Multiplanar reformatted 3D coronary MRA of a healthy volunteer. (A) The LAD, the LCX, and the proximal part of the RCA are displayed. (B) Another view (RCA) of the same acquisition. The data were acquired in five consecutive breathholds of 15-sec duration each.

in five consecutive breathholds of approximately 15-sec (15 heart beats) duration each. The LM, LAD, and RCA could be reliably identified in all subjects. The average measured length was 11.6 ± 1 mm for the LM and 47.6 ± 17.9 mm (range, 30–83 mm) for the LAD. For the LCX, a total length of 22.7 ± 8.2 mm was found for three subjects. The vessel could not be visualized in the other two subjects. The total continuously visualized length of the RCA was 74.6 ± 4.7 mm (range, 68–85 mm).

The left and right coronary system could be consistently visualized with good blood-muscle contrast as shown in Figs. 3 and 4. In Fig. 3 the left (A) and right (B) coronary systems of one subject are displayed. Both reconstructions originate from the same 3D dataset. In Fig. 3A, the LM and the LAD are displayed in a contiguous segment 8.3 cm long. In the same image, a 3.5-cm contiguous segment of the LCX can be seen. The RCA is seen in Fig. 3B. No evidence of discontinuities were observed in the images of Fig. 3. Specifically, no local signal voids were induced by the navigator located at the basal anterior free wall of the LV. In Fig. 4 (A–D), multiplanar reformatted coronary MRAs as acquired in four other individuals are displayed in different reconstructed views. Consistent with the example of Fig. 3, no discontinuities or navigator-induced signal voids can be observed.

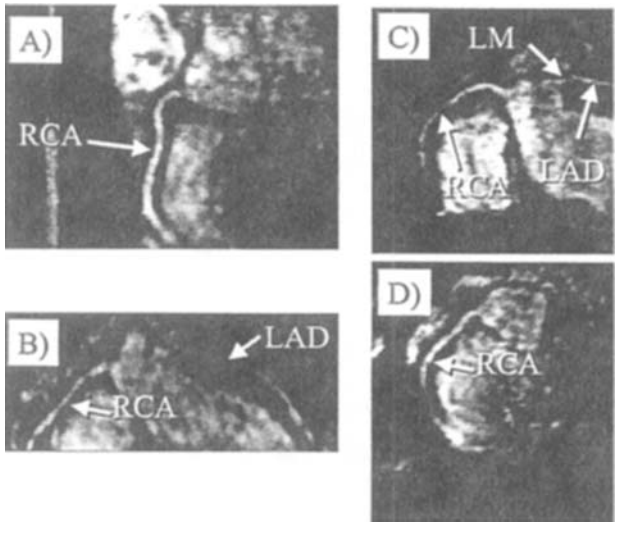

Figure 4. Multiple views of the RCA (A–D), the LAD (B and C), and the LM (C) as acquired in four different healthy subjects.

DISCUSSION

Combining multiple breathholds with real-time navigator tracking allows the advantages of both methods to be exploited. Although navigators alone allow for respiratory gating, image quality only approaches that of a breathhold (19). This combination enables one to increase the information acquired during a single breathhold without introducing blurring or discontinuities due to registration errors or diaphragmatic drift in the images. Splitting of the 3D volume into smaller 3D slabs may also help to enhance the inflow contrast in late diastole, a period of increased coronary flow (20).

However, boundary conditions defined by breathhold duration, image resolution, and the duration of the acquisition window (intrinsic myocardial motion) still do apply (18). Therefore, the application of ultrafast imaging techniques is crucial to take full advantage of breathhold splitting. Using an interleaved segmented EPI approach, the echo time can be shortened with respect to EPI methods where the same number of profiles are acquired in one shot. Therefore, this technique has a potential to be less sensitive to image artifacts (flow, motion) as induced by prolonged echo times. With respect to segmented k-space acquisition schemes in which one k-line is acquired per RF excitation, TFE-EPI allows shortening of the acquisition window (if the same number k-lines is acquired per shot) because the duration of the shot does not primarily depend on TR. In the slice selection direction, an improvement in resolution may be preferred and is associated with a reduced thickness per 3D slab and thus a reduced overall coverage of the total 3D volume. This reduced coverage can be compensated by an in-

crease in the number of acquired 3D slabs, which only affects the number of breathholds but not the duration of the breathhold.

A powerful alternative to breathhold segmenting is the acquisition of multiple 3D volumes per cardiac cycle (21). However, signal voids in the regions of overlapping 3D slabs may be a limitation to noncontrast agent techniques, and image data from the different slabs may not refer to the same contractile state of the myocardium. In the present multislab implementation, the RF excitations of the different subvolumes are separated by the relatively long breathing recovery period. Thus, signal voids in the regions of overlap may be avoided (T1 relaxation and inflow). Furthermore, the data from each slab are acquired at the same time in the cardiac cycle, during a relatively short acquisition window of 70-msec duration. Thus, the 3D data of the different slabs always refer to the same contractile state of the myocardium.

For prospective adaptive navigator correction without gating, scan efficiency is not related to the width of a navigator window (19). Even though the technique may compensate for the effects of diaphragmatic drift and inconsistent depths of subsequent breathhold positions, navigator tracking without gating is not likely to be successful for free-breathing coronary MRA (10,19). However, this remains to be further investigated in the presence of a 2D selective navigator localized at the base of the left ventricle.

The use of the 2D selective navigator excitation allows localization of the navigator in very close proximity to the coronary arteries without introducing local signal voids that may compromise the obtained image information. Furthermore, no model relating diaphragmatic and cardiac motion (11) has to be used.

The current technique has the potential to screen for anomalous coronary arteries in a short time, making it suitable as a part of a larger clinical MR examination. In addition, the technique may also be applied as a scout scan, allowing an accurate definition of imaging planes for subsequent high-resolution coronary MRA.

CONCLUSIONS

By combining prospective real-time navigator slice correction and ultrafast imaging techniques, the acquisition of large 3D coronary MRA data sets can be acquired in multiple short breathholds, whereas the disadvantageous effects of nonconsistent end-expiratory positions and diaphragmatic drift are suppressed. Thus, coverage of extensive portions of the coronary system is possible with multiple shorter breathholds. Because only navigator tracking but no gating is used, scan duration and hence breathhold duration is consistent for all individuals. As a consequence, the advantages of breathhold techniques are preserved and the applicability to patients may be further enhanced.

REFERENCES

1. Edelman RR, Manning WJ, Burstein D, and Paulin S. Coronary arteries: breath-hold MR angiography. *Radiology*, 1991; 181:641–643.
2. Manning WJ and Edelman RR. Magnetic resonance coronary angiography. *Magn Reson Q*, 1993; 9:131–151.
3. Manning WJ, Li W and Edelman RR. A preliminary report comparing magnetic resonance coronary angiography with conventional angiography. *N Engl J Med*, 1993; 328:828–832.
4. Bornert P and Jensen D. Coronary artery imaging at 0.5 T using segmented 3D echo planar imaging. *Magn Reson Med*, 1995; 34:779–785.
5. Li D, Kaushikkar S, Haacke EM, Woodard PK, Dhawale PJ, Kroeker RM, Raub G, Kuginuki Y and Gutierrez FL. Coronary arteries: three-dimensional MR imaging with retrospective respiratory gating. *Radiology*, 1996; 201: 857–863.
6. Wang Y, Rossman PJ, Grimm RC, Wilman AH, Riederer SJ and Ehman RL. 3D MR angiography of pulmonary arteries using real-time navigator gating and magnetization preparation. *Magn Reson Med*, 1996; 36:579–587.
7. Stuber M, Botnar RM, Danias PG, Kissinger KV and Manning WJ. Submillimeter 3D coronary MRA using real-time navigator correction: comparison of navigator locations. *Radiology* (in press).
8. Davis SF, Kannam JP, Wielopolski P, Edelman RR, Anderson TJ and Manning WJ. Magnetic resonance coronary angiography in heart transplant recipients. *J Heart Lung Transpl*, 1996; 15:580–586.
9. Liu YL, Riederer SJ, Rossman PJ, Grimm RC, Debbins JP and Ehman RL. A monitoring, feedback, and triggering system for reproducible breath-hold MR imaging. *Magn Reson Med*, 1993; 30:507–511.
10. Taylor AM, Jhooti P, Wiesmann F, Keegan J, Firmin DN and Pennell DJ. MR navigator-echo monitoring of temporal changes in diaphragm position: implications for MR coronary angiography. *J Magn Reson Imaging*, 1997; 7: 629–636.
11. Wang Y, Riederer SJ and Ehman RL. Respiratory motion of the heart: kinematics and the implications for the spatial resolution in coronary imaging. *Magn Reson Med*, 1995; 33:713–719.
12. Danias PG, Stuber M, Botnar RM, Kissinger KV, Chuang ML and Manning WJ. Navigator assessment of breath-

hold duration: impact of supplemental oxygen and hyperventilation. *AJR Am J Roentgenol*, 1998; 171:395–397.
13. McConnell MV, Khasgiwala VC, Savord BJ, et al. Prospective adaptive navigator correction for breath-hold MR coronary angiography. *Magn Reson Med*, 1997; 37: 148–152.
14. Chuang ML, Chen MH, Khasgiwala VC, McConnel MV, Edelman RR and Manning WJ. Adaptive correction of imaging plane position in segmented k-space cine cardiac MRI. *J Magn Reson Imaging*, 1997; 7:811–814.
15. McKinnon GC. Ultrafast interleaved gradient-echo-planar imaging on a standard scanner. *Magn Reson Med*, 1993; 30:609–616.
16. Brittain JH, Hu BS, Wright GA, Meyer CH, Macovski A and Nishimura DG. Coronary angiography with magnetization-prepared T2 contrast. *Magn Reson Med*, 1995; 33:689–696.
17. Botnar RM, Stuber M, Danias PG, Kissinger KV and Manning WJ. Improved coronary artery definition with T2-weighted free-breathing 3D-coronary MRA. *Circulation* (in press).
18. Hofman MB, Wickline SA and Lorenze CH. Quantification of in-plane motion of the coronary arteries during the cardiac cycle: implications for acquisition window duration for MR flow quantification. *J Magn Reson Imaging*, 1998; 8:568–576.
19. Danias PG, McConnell MV, Khasgiwala VC, Chuang ML, Edelman RR and Manninng WJ. Prospective navigator correction of image position for coronary MR angiography. *Radiology*, 1997; 203:733–736.
20. Davis WL, Warnock SH, Harnsberger HR, Parker DL and Chen CX. Intracranial MRA: single volume vs. multiple thin slab 3D time-of-flight acquisition. *J Comput Assist Tomogr*, 1993; 17:15–21.
21. Goldfarb JW and Edelman RR. Coronary arteries: breath-hold, gadolinium-enhanced, three-dimensional MR angiography, *Radiology*, 1998; 206:830–834.